Draft version February 9, 2011
Preprint typeset using LaTeX style emulateapj v. 11/10/09

THE DISTANCE TO THE MASSIVE ECLIPSING BINARY LMC-SC1-105 IN THE LARGE MAGELLANIC CLOUD

Alceste Z. Bonanos[1], Norberto Castro[1], Lucas M. Macri[2], Rolf-Peter Kudritzki[3,4]

Draft version February 9, 2011

ABSTRACT

This Letter presents the first distance measurement to the massive, semi-detached, eclipsing binary LMC-SC1-105, located in the LH 81 association of the Large Magellanic Cloud (LMC). Previously determined parameters of the system are combined with new near-infrared photometry and a new temperature analysis to constrain the reddening toward the system, and determine a distance of 50.6 ± 1.6 kpc (corresponding to a distance modulus of 18.52 ± 0.07 mag), in agreement with previous eclipsing binary measurements. This is the sixth distance measurement to an eclipsing binary in the LMC, although the first to an O-type system. We thus demonstrate the suitability of O-type eclipsing binaries (EBs) as distance indicators. We suggest using bright, early-type EBs to measure distances along different sight lines, as an independent way to map the depth of the LMC and resolve the controversy about its three-dimensional structure.

Subject headings: binaries: eclipsing – stars: distances – distance scale – stars: individual (OGLE J053448.26-694236.4) – stars: fundamental parameters – galaxies: individual (LMC)

1. INTRODUCTION

As one of the nearest galaxies to the Milky Way, the Large Magellanic Cloud (LMC) has naturally been an attractive first rung for the Extragalactic Distance Scale. The *HST* Key Project (Freedman et al. 2001) adopted a distance modulus $\mu = 18.50 \pm 0.10$ mag (corresponding to a distance of 50.1±2.4 kpc) to the LMC, which has since become the consensus in the community. Schaefer (2008) pointed out that overestimation of error bars and band-wagon effects are present in the literature, with pre-2001 LMC distance measurements yielding values between 18.1 and 18.8 mag (see Benedict et al. 2002), and post-2001 values clustering around the Key Project value. Given that different systematic errors accompany each method, a careful comparison of the distances resulting from different methods is necessary to characterize them. Furthermore, there is increasing evidence for substantial and complex vertical structure in the disk of the LMC (see review by van der Marel 2006) from studies of red clump stars (Olsen & Salyk 2002; Subramanian & Subramaniam 2010), Cepheid variables (Nikolaev et al. 2004) and RR Lyrae stars (Pejcha & Stanek 2009), which demands further exploration.

The only direct, geometrical method available for measuring distances to stars in the LMC is with eclipsing binaries (EBs). In particular, the light curve provides the fractional radii of the components, the radial velocity semi-amplitudes determine the masses and size of the orbit, which together with the effective temperature determination (e.g. by comparison with synthetic spectra), yield luminosities and therefore distances (see reviews by Andersen 1991; Torres et al. 2010). The EB distance method has so far been applied to four early-B type systems (Guinan et al. 1998; Ribas et al. 2002; Fitzpatrick et al. 2002, 2003) and one G-type giant system (Pietrzyński et al. 2009) in the LMC, with individual uncertainties ranging from 1.2 to 2.2 kpc. Four of these systems are located within the bar of the LMC and their individual distances are consistent with the quoted uncertainties, yielding an error-weighted mean value of 49.4 ± 1.1 kpc. A fifth system, located several degrees away in the north-east quadrant of the disk of the LMC, gives a 3σ shorter distance of 43.2 ± 1.8 kpc.

Figure 1 shows the spatial distribution of all known EBs from the OGLE II (Wyrzykowski et al. 2003) and MACHO (Derekas et al. 2007; Faccioli et al. 2007) microlensing surveys of the LMC, and the systems with measured distances, overlaid onto the *Spitzer* SAGE image in the IRAC 3.6 μm band (Meixner et al. 2006). A magnitude cut ($V < 17$ mag) and period cut (> 1.5 days) were both applied to the EB catalogs to reject foreground systems and faint systems whose immediate follow up is unrealistic or impossible. The detached EBs selected by Michalska & Pigulski (2005) among the OGLE II systems as being most suitable for distance determination are also shown. Both the H I kinematic center (Kim et al. 1998) and the dynamical center (or center of the bar; van der Marel et al. 2002) are overplotted, as is the line of nodes ($\Theta = 129.^\circ9 \pm 6.^\circ0$ deg; van der Marel et al. 2002).

Motivated by the evidence for vertical structure in the LMC and the one discrepant EB distance, we proceed to compute the distance to LMC-SC1-105[5]. LMC-SC1-

[1] Institute of Astronomy & Astrophysics, National Observatory of Athens, I. Metaxa & Vas. Pavlou St., P. Penteli, 15236 Athens, Greece; bonanos@astro.noa.gr, norberto@noa.gr
[2] George P. and Cynthia Woods Mitchell Institute for Fundamental Physics and Astronomy, Department of Physics & Astronomy, Texas A&M University, 4242 TAMU, College Station, TX 77843-4242, USA; lmacri@physics.tamu.edu
[3] Institute for Astronomy, University of Hawaii, 2680 Woodlawn Dr., Honolulu, HI 96822, USA; kud@ifa.hawaii.edu
[4] Max-Planck-Institute for Astrophysics, Karl-Schwarzschild-Str. 1, D-85741 Garching, Germany.

[5] Or OGLE J053448.26-694236.4 = MACHO 81.8881.21 = LH 81-72.

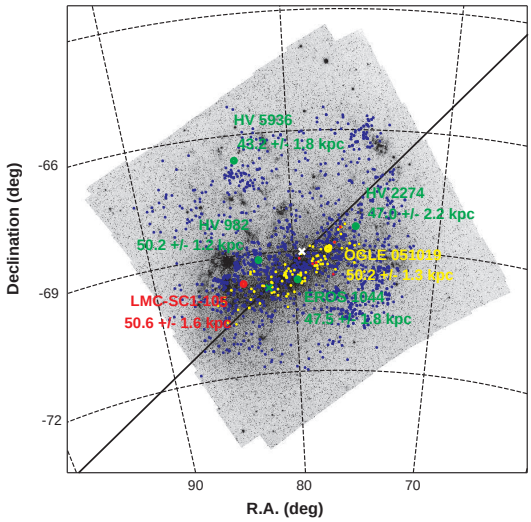

FIG. 1.— Spatial distribution of known EBs from OGLE II and MACHO (blue circles) on the *Spitzer* 3.6μm image of the LMC. EBs with measured distances are labeled. Yellow circles mark the most suitable detached EBs for distance determination (Michalska & Pigulski 2005); red circles mark the OGLE II binaries we plan to measure distances to next. The H I kinematic center (white "x") from Kim et al. (1998) and the dynamical center or center of the bar (green "x") from van der Marel et al. (2002) are labeled; the solid line corresponds to the line of nodes (van der Marel et al. 2002). Coordinates are given for J2000.

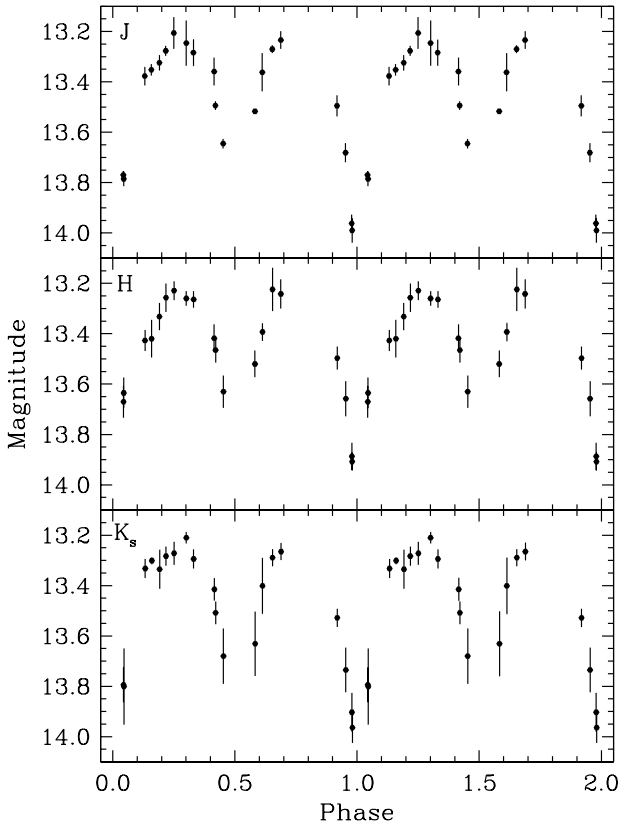

FIG. 2.— Phased CPAPIR JHK_s-band light curves of LMC-SC1-105.

105 is a massive, semi-detached, short period ($P = 4.25$ days) O-type system, with component masses of $M_1 = 30.9 \pm 1.0$ $M_\odot$, $M_2 = 13.0 \pm 0.7$ $M_\odot$, and radii of $R_1 = 15.1 \pm 0.2$ $R_\odot$, $R_2 = 11.9 \pm 0.2$ $R_\odot$ (determined by Bonanos 2009). The very accurate measurement of the radii ($< 2\%$) renders the system suitable for a distance determination, given that EB distances are independent of the usual distance ladder and therefore important checks for other methods. However, accurate radii are not sufficient for an accurate distance. Accurate fluxes (i.e. effective temperatures) and extinction estimates are also needed, therefore this Letter sets out to determine these quantities and obtain the distance. Specifically, Section 2 presents new near-infrared photometry of LMC-SC1-105, Section 3 an analysis of the spectra with state-of-the-art model atmospheres, Section 4 the distance determination, and finally, Section 5 a discussion of our results.

2. NEAR-INFRARED DATA

This study makes use of JHK_s observations of LMC-SC1-105 obtained with the CPAPIR camera (Artigau et al. 2004) at the CTIO 1.5-m, as part of a synoptic survey of Cepheid variables in the LMC (L. M. Macri et al. 2011, in prep.). The EB was observed at 20 different epochs on 11 nights between 2006 November 5 and 2007 December 2. Time-series PSF photometry was carried out using DAOPHOT and ALLFRAME (Stetson 1987, 1994). Photometric zeropoints were determined using $\sim 2,500$ stars from the 2MASS Point Source Catalog, located within $15'$ of the system and with $10.5 < K_s < 13.5$ mag, while color terms were derived using nearly 5×10^5 2MASS stars across the entire bar of the LMC. Figure 2 shows the calibrated, phased light curves of LMC-SC1-105. We calculated error-weighted out-of-eclipse mean magnitudes of $J = 13.22 \pm 0.04$, $H = 13.27 \pm 0.04$ and $K_s = 13.26 \pm 0.04$ mag.

3. EFFECTIVE TEMPERATURE ANALYSIS

An accurate distance measurement to LMC-SC-105 requires an accurate flux determination for its binary components. We proceed to refine the effective temperatures estimated by Bonanos (2009)[6] with the state-of-the-art, NLTE stellar atmosphere code FASTWIND (Santolaya-Rey et al. 1997; Puls et al. 2005), which includes the effects of stellar winds and spherical atmospheric extension.

The analysis involves a direct comparison between the helium lines, which are the main temperature diagnostics at these spectral types, plus Hα, to constrain the stellar wind, with a complete FASTWIND model grid designed to study O-type stars at the metallicity of the LMC. The grid was developed within the FLAMES-II collaboration (Evans et al. 2010) and constructed at the Instituto de Astrofísica de Canarias. Specifically, we derived the set of models that provide the lowest χ^2, using Hα and the 10 strongest He I and He II lines available[7]. The synthetic models were downgraded to the instrumental resolution of the observed spectra and the projected ro-

[6] $T_{\rm eff1} = 35 \pm 2.5$kK, $T_{\rm eff2} = 32.5 \pm 2.5$kK, for $\log(g) = 3.50$ (fixed), from best fit TLUSTY models (Lanz & Hubeny 2003).

[7] He I $\lambda\lambda$4026, 4143, 4471, 4713, 4922, 5015, 5875 and He II $\lambda\lambda$4200, 4541, 5411.

tational velocities $v \sin i$ were refined to 160 km s^{-1} and 120 km s^{-1}, for the primary and secondary component, respectively. We fixed the surface gravities to the values determined by Bonanos (2009): $\log(g_1) = 3.57 \pm 0.02$ and $\log(g_2) = 3.40 \pm 0.03$[8]. In practice, we rounded the values to the first decimal point, to match the 0.1 dex step size of the grid. The χ^2 method provides the stellar parameters and their corresponding errors.

The technique was applied to the two highest S/N spectra of LMC-SC1-105 (see Bonanos 2009), obtained at phases 0.27 and 0.75, i.e. at the first and second quadratures. Both phases yielded the same temperature for each component, within the errors. Specifically, at first quadrature, we found best fit values of $T_{eff1} = 36100 \pm 1000$ K, $T_{eff2} = 33200 \pm 800$ K, while at the second quadrature $T_{eff1} = 35700 \pm 1100$ K, $T_{eff2} = 33100 \pm 900$ K. Figures 3 and 4 show the best fit FASTWIND models, plus the effects of the temperature errors in the profiles. The synthetic models, which only include transitions of H I, He I and He II, provide a good match to the observed spectra. Despite not including the Balmer lines in the analysis (except Hα), the wings of these lines are in good agreement with the models, confirming the accuracy of the $\log(g)$ determination from the EB analysis.

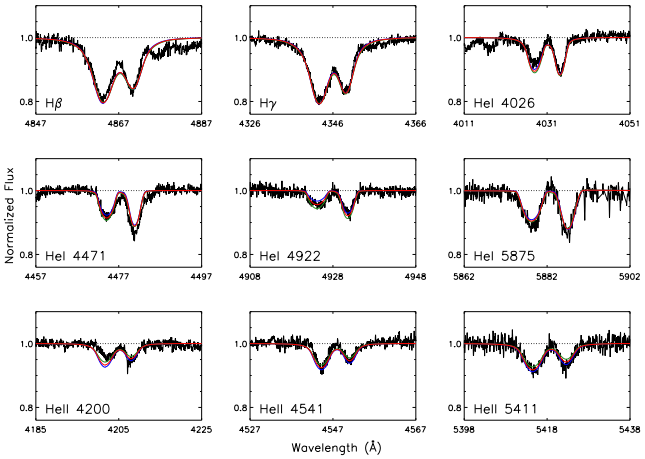

FIG. 3.— Best fit FASTWIND model (red) of LMC-SC1-105, at the first quadrature. The blue (green) lines correspond to models with the best fit T_{eff} plus (minus) the 1σ error. The set of lines with smaller Doppler shifts corresponds to the primary.

Bonanos (2009) reported changes of the spectral types with phase due to the Struve-Sahade effect (Stickland 1997), the largest being from O7V to O8V for the primary, which would have an impact on the temperature of ~ 2000 K (Martins et al. 2005). Our analysis, however, does not yield any remarkable differences in temperature between the two quadratures. The reason for this is that the classification criteria (Walborn & Fitzpatrick 1990) hinge on the lines He II λ4541, He I λ4471, He II λ4200, and He I+II λ4026, while the FASTWIND analysis averaged over 10 He I and He II lines in the spectrum. The imperfect fits of He II λ4200 and He I λ4471 by the models (see Figure 3), are consistent with a spectral type change.

[8] Note, the $\log(g)$ error bars given in Table 5 of Bonanos (2009) incorrectly correspond to the errors in g.

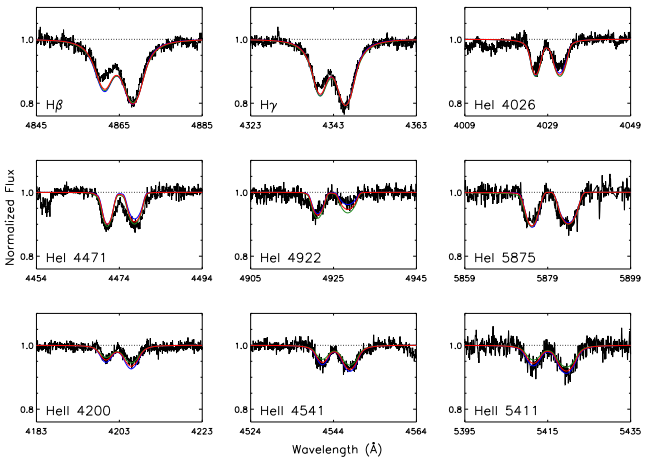

FIG. 4.— Same as Figure 3, but for the second quadrature. The set of lines with larger Doppler shifts corresponds to the primary.

At phase 0.75, the secondary star shows important deviations in the cores of Hβ and Hγ from the model (see Figure 4), which might be due to excess emission arising from the slow mass transfer or the distorted line profiles of Roche lobe-filling stars (see Bitner & Robinson 2006). Nonetheless, the rest of the He I and He II lines are well modeled within the errors. Some of the He II lines (e.g. He II λ4541) might indicate a slightly higher temperature, however these differences lie within the errors.

4. DISTANCE

The flux f_λ measured at Earth at a certain wavelength λ from a binary at distance d is given by

$$f_\lambda = \frac{1}{d^2}\left(R_1^2\, F_{1,\lambda} + R_2^2\, F_{2,\lambda}\right) \times 10^{-0.4\, A(\lambda)}, \qquad (1)$$

where R_1 and R_2 are the radii of the two stars and $F_{1,\lambda}$ and $F_{2,\lambda}$ the surface fluxes. The total extinction $A(\lambda)$ is a function of the reddening $E(B-V)$, the normalized extinction curve $k(\lambda - V) \equiv E(\lambda - V)/E(B-V)$ and the ratio of total to selective extinction in the V band, $R_V \equiv A(V)/E(B-V)$:

$$A(\lambda) = E(B-V)\left[k(\lambda - V) + R_V\right]. \qquad (2)$$

Having measured the temperatures of the stars from the spectra, we computed fluxes and fit to the observed magnitudes, using Equation 1 and the best-fit FASTWIND model atmospheres for each quadrature determined above. Note that we used the mean radii[9] of the stars instead of their volume radii as better approximations to compute their projected surface areas.

Following the procedure outlined in Bonanos et al. (2006) for the detached EB in M33, we calculated synthetic photometry of the composite spectrum over the appropriate Johnson-Cousins optical filter functions as defined by Bessell (1990) and calibrated by Landolt (1992), and the 2MASS filter set. Monochromatic fluxes were measured at the isophotal wavelengths (see Tokunaga & Vacca 2005), which best represent the flux in a passband. We used zeropoints from Bessell et al.

[9] $(r_{pole} + r_{side} + r_{back})/3$

(1998, Appendix A) and Cohen et al. (2003) to convert the fluxes to magnitudes. We reddened the model spectrum using the reddening law parameterization of Cardelli et al. (1989), as prescribed in Schlegel et al. (1998), and simultaneously fit the optical[10] and near-infrared $BVIJHK_s$ photometry. Specifically, we computed the intrinsic $(B-V)_0 = -0.27$ mag from the model atmospheres at the isophotal wavelengths, thus yielding $E(B-V) = 0.11 \pm 0.01$ mag.

The value of R_V was determined as the value that minimized the error in the SED fit over the six photometric bands. For phase 0.27, we found $R_V = 5.8 \pm 0.4$ and for phase 0.75, $R_V = 5.7 \pm 0.4$. The resulting distance to LMC-SC1-105 and thus the LMC bar is 50.6 ± 1.6 kpc ($\mu = 18.52 \pm 0.07$ mag) for the first quadrature and 50.4 ± 1.6 kpc ($\mu = 18.51 \pm 0.07$ mag) for the second quadrature. The distances are identical within errors. Given the better fit of the FASTWIND models to the spectra at first quadrature, we adopt the distance derived for first quadrature. The fit of the reddened model spectrum to the photometry and the residuals of the fit are shown in the upper and lower panels of Figure 5, respectively. The error in the distances was computed by a bootstrap resampling procedure. We repeated the spectral energy distribution (SED) fitting procedure 1000 times for each quadrature, by randomly selecting (using Gaussian sampling) all the parameters within their errors. We adopt the σ of the resulting Gaussian distribution as the uncertainty in the distance.

We tested the robustness of our reddening and distance results, by first fitting the BVI photometry alone, which yielded an identical value for the distance (50.8 ± 1.6 kpc or $\mu = 18.53 \pm 0.07$ mag, with $R_V = 5.7 \pm 0.4$), thus demonstrating the consistency of the near-infrared with the optical photometry. Next, if we fix $R_V = 3.1$, the best fit value for $E(B-V) = 0.18$ mag, resulting in a distance of 51.9 ± 1.6 kpc ($\mu = 18.58 \pm 0.07$ mag), i.e. in agreement with our reported result, within errors. If instead we assume $R_V = 3.1$ and fix $E(B-V) = 0.11 \pm 0.01$ mag (based on our photometry and the model spectra)[11], we would derive a much larger distance of 55.2 kpc ($\mu = 18.71$ mag), which yields a SED fit error of 0.05 mag (versus 0.01 mag) that is inconsistent with the photometry. The validity and implications of the high value of R_V that we have measured are discussed in the following Section.

The error quoted above for R_V was estimated using the Bayesian code CHORIZOS (Maíz-Apellániz 2004). The available $BVIJHK_s$ photometry was given as input, with Teff in the range 33000−36000 K and $\log(g)$ fixed to 3.50, from TLUSTY models. The code yielded best fit mean values (for a single star) of $T_{\rm eff} = 34500 \pm 1100$ K, $R_{\lambda 5495} = 5.4 \pm 0.4$ and $E(\lambda 4405 - \lambda 5495) = 0.10 \pm 0.01$ mag, consistent with the values we derived.

5. DISCUSSION

LMC-SC1-105 is located in the LH 81 association (Massey et al. 2000), near the center of the LMC bar. It contains two early O-type stars and three Wolf-Rayet systems, one of which was recently found to be an EB (Szczygieł et al. 2010). Furthermore, this association resides in the superbubble N 154 (Henize 1956) = DEM 246 (Davies et al. 1976). We have determined a large value of $R_V = 5.8 \pm 0.4$ toward LMC-SC1-105, however, such high values are not uncommon. Cardelli et al. (1989) find $5 < R_V \leq 5.6$ for 6 out of the 29 OB stars in their sample, while Fitzpatrick & Massa (2007) find $R_V > 5$ for 12 out of the 328 stars in their sample. Large values of R_V simply imply larger dust grain sizes, which are expected to occur in dense regions of the interstellar medium due to accretion and coagulation of grains. We therefore conclude that the environment in which LMC-SC1-105 resides has large dust grains.

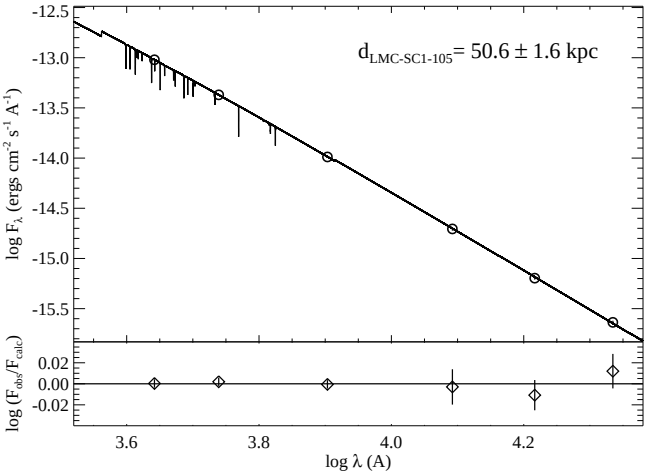

FIG. 5.— Upper panel: fit of the reddened EB model spectrum (for phase 0.27) to the $BVIJHK_s$ photometry. Lower panel: residuals of the SED fit, in terms of the flux ratio. Error bars correspond to the photometric error for each band in flux units. The best fit values of $E(B-V) = 0.11 \pm 0.01$ mag and $R_V = 5.8 \pm 0.4$ yield a distance modulus to the EB and thus the LMC bar of 50.6 ± 1.6 kpc ($\mu = 18.52 \pm 0.07$ mag).

In this Letter, we have determined the distance to LMC-SC1-105 and consequently the LMC bar to be 50.6 ± 1.6 kpc ($\mu = 18.52 \pm 0.07$ mag). The agreement we find with previous EB distances to systems in the bar with different spectral types testifies to the robustness of the EB method and its potential as a powerful, independent distance indicator. Furthermore, it confirms that O-type (and semi-detached) EBs are suitable for distance determination, i.e. that the fluxes predicted by FASTWIND are indeed accurate. EB-based distance determinations to M31 (Ribas et al. 2005; Vilardell et al. 2010) and M33 (Bonanos et al. 2006) can therefore provide an independent absolute calibration of the Extragalactic Distance Scale. Future distance determinations to EBs in the LMC (e.g. those marked in Figure 1), will additionally provide R_V values in different environments of the LMC. Finally, we suggest using bright, early-type EBs to measure distances along different sight lines to the LMC, as an independent way to map its depth and resolve the controversy about its vertical structure.

We are very grateful to S. Símon-Díaz for making available part of his FASTWIND grid at $Z/Z_\odot = 0.4$. L.M.M. thanks Shashi Kanbur and Chow-Choong Ngeow for allowing the use of the CPAPIR data in advance of publication. The CPAPIR survey of the LMC was made possible

[10] $B_{\rm max} = 12.81 \pm 0.01$ mag, $V_{\rm max} = 12.97 \pm 0.01$ mag, $I_{\rm max} = 13.04 \pm 0.01$ mag (Wyrzykowski et al. 2003).

[11] Note, our $E(B-V)$ value is consistent with the range (0.13-0.23 mag) measured by Massey et al. (2000) for 34 stars in LH 81.

by faculty startup funds from the State University of New York at Oswego and Texas A&M University. A.Z.B. and N.C. acknowledge research and travel support from the European Commission Framework Program Seven under a Marie Curie International Reintegration Grant. R.P.K. acknowledges support by the Alexander-von-Humboldt-Foundation and from the National Science Foundation under grant AST-1008797. This research has made use of SAOImage DS9, developed by Smithsonian Astrophysical Observatory.

REFERENCES

Andersen, J. 1991, A&A Rev., 3, 91
Artigau, É., Doyon, R., Vallee, P., et al. 2004, in Society of Photo-Optical Instrumentation Engineers (SPIE) Conference Series, Vol. 5492, Society of Photo-Optical Instrumentation Engineers (SPIE) Conference Series, ed. A. F. M. Moorwood & M. Iye, 1479–1486
Benedict, G. F., McArthur, B. E., Fredrick, L. W., et al. 2002, AJ, 123, 473
Bessell, M. S. 1990, PASP, 102, 1181
Bessell, M. S., Castelli, F., & Plez, B. 1998, A&A, 333, 231
Bitner, M. A. & Robinson, E. L. 2006, AJ, 131, 1712
Bonanos, A. Z. 2009, ApJ, 691, 407
Bonanos, A. Z., Stanek, K. Z., Kudritzki, R. P., et al. 2006, ApJ, 652, 313
Cardelli, J. A., Clayton, G. C., & Mathis, J. S. 1989, ApJ, 345, 245
Cohen, M., Wheaton, W. A., & Megeath, S. T. 2003, AJ, 126, 1090
Davies, R. D., Elliott, K. H., & Meaburn, J. 1976, MmRAS, 81, 89
Derekas, A., Kiss, L. L., & Bedding, T. R. 2007, ApJ, 663, 249
Evans, C. J., Bastian, N., Beletsky, Y., et al. 2010, in IAU Symposium, Vol. 266, IAU Symposium, ed. R. de Grijs & J. R. D. Lépine, 35–40
Faccioli, L., Alcock, C., Cook, K., et al. 2007, AJ, 134, 1963
Fitzpatrick, E. L. & Massa, D. L. 2007, ApJ, 663, 320
Fitzpatrick, E. L., Ribas, I., Guinan, E. F., et al. 2002, ApJ, 564, 260
—. 2003, ApJ, 587, 685
Freedman, W. L., Madore, B. F., Gibson, B. K., et al. 2001, ApJ, 553, 47
Guinan, E. F., Fitzpatrick, E. L., Dewarf, L. E., et al. 1998, ApJ, 509, L21
Henize, K. G. 1956, ApJS, 2, 315
Kim, S., Staveley-Smith, L., Dopita, M. A., et al. 1998, ApJ, 503, 674
Landolt, A. U. 1992, AJ, 104, 340
Lanz, T. & Hubeny, I. 2003, ApJS, 146, 417
Maíz-Apellániz, J. 2004, PASP, 116, 859
Martins, F., Schaerer, D., & Hillier, D. J. 2005, A&A, 436, 1049
Massey, P., Waterhouse, E., & DeGioia-Eastwood, K. 2000, AJ, 119, 2214
Meixner, M., Gordon, K. D., Indebetouw, R., et al. 2006, AJ, 132, 2268
Michalska, G. & Pigulski, A. 2005, A&A, 434, 89
Nikolaev, S., Drake, A. J., Keller, S. C., et al. 2004, ApJ, 601, 260
Olsen, K. A. G. & Salyk, C. 2002, AJ, 124, 2045
Pejcha, O. & Stanek, K. Z. 2009, ApJ, 704, 1730
Pietrzyński, G., Thompson, I. B., Graczyk, D., et al. 2009, ApJ, 697, 862
Puls, J., Urbaneja, M. A., Venero, R., et al. 2005, A&A, 435, 669
Ribas, I., Fitzpatrick, E. L., Maloney, F. P., et al. 2002, ApJ, 574, 771
Ribas, I., Jordi, C., Vilardell, F., et al. 2005, ApJ, 635, L37
Santolaya-Rey, A. E., Puls, J., & Herrero, A. 1997, A&A, 323, 488
Schaefer, B. E. 2008, AJ, 135, 112
Schlegel, D. J., Finkbeiner, D. P., & Davis, M. 1998, ApJ, 500, 525
Stetson, P. B. 1987, PASP, 99, 191
—. 1994, PASP, 106, 250
Stickland, D. J. 1997, The Observatory, 117, 37
Subramanian, S. & Subramaniam, A. 2010, A&A, 520, A24
Szczygieł, D. M., Stanek, K. Z., Bonanos, A. Z., et al. 2010, AJ, 140, 14
Tokunaga, A. T. & Vacca, W. D. 2005, PASP, 117, 421
Torres, G., Andersen, J., & Giménez, A. 2010, A&A Rev., 18, 67
van der Marel, R. P. 2006, in The Local Group as an Astrophysical Laboratory, ed. M. Livio & T. M. Brown, 47–71
van der Marel, R. P., Alves, D. R., Hardy, E., et al. 2002, AJ, 124, 2639
Vilardell, F., Ribas, I., Jordi, C., et al. 2010, A&A, 509, A70
Walborn, N. R. & Fitzpatrick, E. L. 1990, PASP, 102, 379
Wyrzykowski, L., Udalski, A., Kubiak, M., et al. 2003, Acta Astronomica, 53, 1